

MASS TABLE MEAN-FIELD CALCULATIONS

M.V. STOITSOV¹⁻⁴, W. NAZAREWICZ³⁻⁵, J. DOBACZEWSKI⁵

¹ *Institute of Nuclear Research and Nuclear Energy,
Bulgarian Academy of Sciences, Sofia-1784, Bulgaria*

² *Joint Institute for Heavy Ion Research, Oak Ridge, Tennessee 37831*

³ *Physics Division, Oak Ridge National Laboratory, Oak Ridge, Tennessee 37831*

⁴ *Department of Physics, University of Tennessee, Knoxville, Tennessee 37996*

⁵ *Institute of Theoretical Physics, Warsaw University, Hoża 69, PL-00-681
Warsaw, Poland*

The mean-field methods are very successful in describing and predicting properties of nuclei across the chart of the nuclides. Results from recent large-scale Hartree-Fock-Bogoliubov calculations in configuration-space are presented for all even-even nuclei ranging from proton drip line to neutron drip line, with proton numbers $Z = 4, 6, 8, \dots, 108$ using Skyrme forces and contact delta pairing interaction. Predictions of properties of exotic nuclei close to the particle drip lines are discussed.

1. Introduction

The development of experimental facilities that accelerate radioactive ion beams and the new detector technology that is accompanying them^{1,2,3,4} has opened up a possibility to study the properties of nuclei very far from the valley of beta stability, all the way out to the particle drip lines.

A proper theoretical description of such weakly bound systems requires a careful treatment of the asymptotic part of the nucleonic density. An appropriate framework for is the Hartree-Fock-Bogoliubov (HFB) in the coordinate representation^{5,6,7}. This method has been used extensively in the treatment of spherical systems but, is much more difficult to implement for systems with deformed equilibrium shapes^{8,9}.

In the absence of reliable coordinate-space solutions to the deformed HFB equations, it is useful to consider instead the configuration-space approach, whereby the HFB solution is expanded in a single-particle basis. There have been many configuration-space HFB calculations performed in a harmonic oscillator (HO) basis, either employing Skyrme forces or the Gogny effective interaction^{10,11,12,13}, or using a relativistic Lagrangian¹⁴.

For nuclei at the drip lines, however, the HFB+HO expansion converges slowly as a function of the number of oscillator shells⁷, producing wave functions that decrease too steeply at large distances.

An alternative approach that has recently been proposed is to expand the quasiparticle HFB wave functions in a complete set of transformed harmonic oscillator (THO) basis states^{15,16,17}, obtained by applying a local-scaling coordinate transformation (LST)^{19,20} to the standard HO basis. Applications of this HFB+THO methodology have been reported both in the non-relativistic¹⁵ and relativistic domains¹⁷. In all of these calculations, specific global parameterizations were employed for the scalar LST function that defines the THO basis. There are several limitations in such an approach, however. For example, the minimization procedure that is needed in such an approach to optimally define the basis parameters is computationally very time consuming, making it very difficult to apply the method systematically to nuclei across the periodic table.

Recently, a new prescription for choosing the THO basis has been proposed¹⁸. For a given nucleus, the new prescription requires as input the results from a relatively simple HFB+HO calculation, with no variational optimization. The resulting THO basis leads to HFB+THO results that almost exactly reproduce the coordinate-space HFB results for spherical nuclei⁶ and they are of comparable quality to available results for axially deformed nuclei⁸.

Because the new prescription requires no variational optimization of the LST function, it can be applied in systematic studies of nuclear properties. In the present study, we report the results of HFB+THO calculations performed for all particle-bound even-even nuclei with $Z \leq 108$ and $N \leq 188$. The mass charts have been calculated with and without the Lipkin-Nogami prescription for an approximate particle number projection, followed by an exact particle number projection after the variation.

The structure of the paper is as follows. In Sec. 2, we briefly review the HFB theory. In Sec. 3, we introduce the THO basis and then, in Sec. 4, formulate the prescription for the LST function. The results of systematic calculations are illustrated in Sec. 5. Conclusions are presented in Sec. 6.

2. Hartree-Fock-Bogoliubov Theory

HFB is a variational theory that treats in a unified fashion mean-field and pairing correlations²¹. The HFB equations can be written in a matrix form

as

$$\begin{pmatrix} h - \lambda & \Delta \\ -\Delta^* & -h^* + \lambda \end{pmatrix} \begin{pmatrix} U_n \\ V_n \end{pmatrix} = E_n \begin{pmatrix} U_n \\ V_n \end{pmatrix}, \quad (1)$$

where E_n are the quasiparticle energies, λ is the chemical potential, $h = t + \Gamma$, and Δ are the HF Hamiltonian and the pairing potential, respectively, and U_n and V_n are the upper and lower components of the quasiparticle wave functions.

In coordinate representation, the HFB approach consists of solving (1) as a set of integro-differential equations with respect to the amplitudes $U(E_n, \mathbf{r})$ and $V(E_n, \mathbf{r})$. The HFB continuum is discretized by putting the system in a large box with appropriate boundary conditions⁷.

In the configurational approach, the HFB equations are solved by matrix diagonalization within a chosen set of single-particle basis wave functions ψ_α with appropriate symmetry properties. The nuclear characteristics of interest are determined by the matrix elements of the density matrix and pairing tensor

$$\begin{aligned} \rho_{\alpha\beta} &= \sum_{0 \leq E_n \leq E_{\max}} V_{\alpha n}^*(E_n) V_{\beta n}(E_n), \\ k_{\alpha\beta} &= \sum_{0 \leq E_n \leq E_{\max}} V_{\alpha n}^*(E_n) U_{\beta n}(E_n). \end{aligned} \quad (2)$$

In configuration-space calculations, all quasiparticle states have discrete energies E_n .

3. Transformed Harmonic Oscillator Basis

Suppose $\{\varphi_\alpha(\mathbf{r})\}$ represents the complete set of HO single-particle wave functions depending on the spatial coordinate \mathbf{r} and oscillator lengths $\{L_x, L_y, L_z\}$. One can introduce a LST of the three-dimensional vector space

$$\mathbf{r} \longrightarrow \mathbf{r}' \equiv \mathbf{r}'(\mathbf{r}) = \frac{\mathbf{r}}{R} f(R), \quad (3)$$

where R is the referent surface

$$R = \sqrt{\frac{x^2}{L_x^2} + \frac{y^2}{L_y^2} + \frac{z^2}{L_z^2}}. \quad (4)$$

The LST function $f(R)$ should have quite general mathematical properties ensuring that (3) is a valid invertible transformation of the three-dimensional space.

When one applies LST (3) to the HO set of wave functions, one obtains another set of THO single-particle wave functions

$$\psi_{\alpha}(\mathbf{r}) = \sqrt{\frac{f^2(R)}{R^2} \frac{\partial f(R)}{\partial R^2}} \varphi_{\alpha} \left(\frac{r}{R} f(R) \right). \quad (5)$$

Due to the Jacobian of the LST entering Eq.(5), the THO wave functions are automatically orthonormalized. They have an asymptotic behavior

$$\psi_{\alpha}(r \rightarrow \infty) \sim \exp \left[-\frac{1}{2} f^2(R) \right], \quad (6)$$

which suggests that if the LST function satisfies the asymptotic conditions

$$f(R) = \begin{cases} R & \text{for small } R, \\ \sqrt{\kappa R} & \text{for large } R, \end{cases} \quad (7)$$

then the THO wave functions at small distances are identical to the HO wave functions, while at large distances they have the exponential asymptotic behavior.

In other words, the LST (3) generates, from a given complete set of HO wave functions, another orthonormal and complete set of THO wave functions (5) depending on an almost-arbitrary scalar LST function $f(R)$. The freedom in the choice of $f(R)$ provides great flexibility in the THO set $\{\psi_{\alpha}(\mathbf{r})\}$, and this opens up the possibility of improving on undesirable properties of the initial set. In particular, the use of the LST in THO can modify the incorrect Gaussian asymptotic properties of deformed HO wave functions.

4. Local-Scaling Transformation Function

The starting point of defining the LST function $f(R)$ is to carry out a standard HFB+HO calculation for the nucleus of interest, thereby generating an $\ell=0$ component

$$\bar{\rho}(r) = \int_0^{\pi/2} \bar{\rho}(r, \theta) P_{\ell=0}(\cos(\theta)) \sin(\theta) d\theta \quad (8)$$

of the (generally deformed) HO local density $\bar{\rho}(r, \theta)$. Inspecting the density (8), one can conclude that its logarithmic derivative $\bar{\rho}'/\bar{\rho}$ exhibits a well-defined minimum near some point R_{min} in the asymptotic region. The comparison shows that the HFB+HO densities and their logarithmic derivatives are in almost perfect agreement with the coordinate-space HFB results up to R_{min} and, therefore, the HFB+HO densities are numerically reliable up

to that point. The value of the density decay constant k emerging from HFB+HO calculations is also in agreement with the coordinate-space HFB results.

Beyond the point R_{min} , however, the logarithmic derivative $\bar{\rho}'/\bar{\rho}$ starts to oscillate around the coordinate-space HFB logarithmic density derivative which smoothly approaches the constant value k . As a result, the logarithmic derivative of the HFB+HO density is very close to the coordinate-space result around the midpoint $R_m = (R_{max} - R_{min})/2$, where R_{max} is the position of the first maximum of the logarithmic derivative for $r > R_{min}$. Beyond the point R_m , the HFB+HO solution $\bar{\rho}(r)$ fails to capture the physics of the coordinate-space results, especially in the far asymptotic region. It is this incorrect large- r behavior that one tries to cure by introducing the THO basis.

To this end, making use of the WKB asymptotic solution of the single-particle Schrödinger equation and assuming that beyond the classical turning point only the state with the lowest decay constant k contributes to the local density, one can introduce the following approximate local density distribution

$$\tilde{\rho}(r) = \begin{cases} \bar{\rho}(r) & \text{for } r \leq R_{min} \\ A e^{-b r} \exp \left[-\frac{a}{r^s} \left(\frac{a r^3}{3-s} - \frac{2 r^2 R_{min}}{2-s} + \frac{r R_{min}^2}{1-s} \right) \right] & \text{for } R_{min} \leq r \leq R_{max} \\ B \frac{\exp \left[-2 \int^r \sqrt{\kappa^2 + \frac{C}{r^2} + \frac{2m}{\hbar^2} \frac{Ze^2}{r}} dr \right]}{r^2 \sqrt{\kappa^2 + \frac{C}{r^2} + \frac{2m}{\hbar^2} \frac{Ze^2}{r}}} & \text{for } r \geq R_{max} \end{cases} \quad (9)$$

where $\bar{\rho}(r)$ is the HFB+HO density (8), the coefficients A and B are determined from the matching condition for the density at points R_{min} and R_{max} , respectively, while the constants a and b , and the power s , are determined from the condition that the logarithmic derivative $\tilde{\rho}'/\tilde{\rho}$ and its first derivative are smooth functions at points R_{min} and R_{max} . The value of C is fixed by the requirement that the logarithmic derivative of (9) coincides at the mid point R_m with the $\ell=0$ component of the HFB+HO density. The density $\tilde{\rho}(r)$ should also be normalized to the appropriate particle number.

Since Eq. (9) approximates HFB local densities fairly well for all nuclei, the next step is to define the LST function so that it transforms the HFB+HO density (8) into the density of Eq. (9). This requirement leads

to the following first-order differential equation,

$$\tilde{\rho}(r) = \frac{f^2(R)}{R^2} \frac{\partial f(R)}{\partial R} \bar{\rho} \left(\frac{r}{R} f(R) \right), \quad (10)$$

which, for the initial condition $f(0) = 0$, can always be solved for $f(R)$.

Once the LST function has been obtained, one needs simply to diagonalize the HFB matrices in the corresponding THO basis. Most importantly, no other information is required to construct the THO basis than the results of a standard HFB+HO calculation. As a consequence, one is able to systematically treat large sets of nuclei within a single calculation.

5. Numerical Example

In this section, we present the results of HFB+THO calculations performed for all the particle-bound even-even nuclei with $Z \leq 108$ and $N \leq 188$. We have used the SLy4 Skyrme force parametrization²³ in the particle-hole channel and an intermediate (mixed) contact pairing force²³ in the pairing channel.

For a given mass number A , calculations were carried out for increasing (decreasing) $N - Z$ up to the nucleus with positive neutron (proton) Fermi energy. Moreover, three independent sets of calculations were performed assuming initial wave functions to correspond to oblate, spherical, and prolate shapes. The lowest of the local minima that were found for a given nucleus was then identified with the ground-state solution. Mass charts have been calculated with and without the Lipkin-Nogami prescription for an approximate particle number projection, followed by an exact particle number projection after the variation.

The results for the ground-states of all even-even nuclei with negative Fermi energies, $\lambda_n < 0$ and $\lambda_p < 0$, are illustrated in Fig. 1. It is interesting to note from Fig. 1(a) that there are fairly large regions of nuclei far from stability with oblate shapes in their ground state. Nonetheless, it remains the case for nuclei far from stability, as for nuclei in or near the valley of stability, that there are more prolate ground states than oblate.

From Fig. 1(b), one can see that there exist numerous particle-bound even-even nuclei (i.e., nuclei with negative Fermi energies) that at the same time have negative two-neutron separation energies. Similar situation, but corresponding to negative two-proton separation energies, is predicted close to the proton-drip line. What this means is that even though these nuclei are bound against one-nucleon emission, they can nevertheless decay spontaneously by emitting two-nucleons. This is related to the fact that

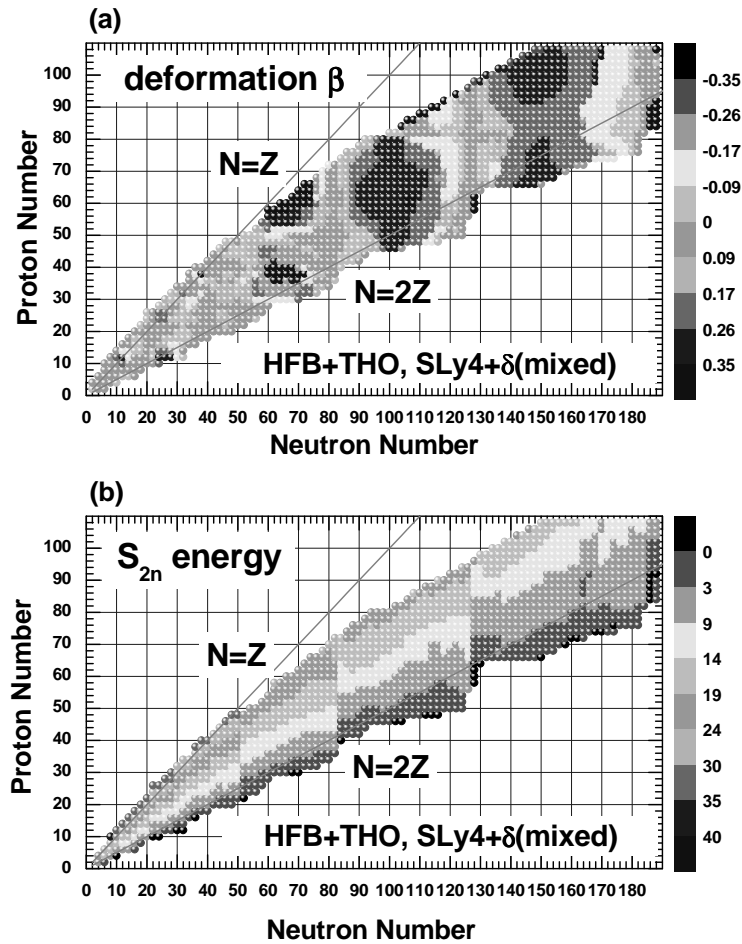


Figure 1. Particle-bound even-even nuclei calculated within the HFB+THO method for the Skyrme SLy4 interaction and mixed contact pairing force within $N_{sh} = 20$ major shells: (a) quadrupole deformations β ; (b) two-neutron separation energies S_{2n} (in MeV).

the HFB Fermi energies are associated with a given configuration or shape. Therefore, they tell us little about particle decays involving shape changes.

6. Concluding Remarks

In this paper, we report the application of an improved version of the configuration-space HFB method expanded in a Transformed Harmonic Oscillator basis. The method can be used reliably in systematic studies of wide ranges of nuclei, both spherical and axially deformed, extending all the way out to nucleon drip lines.

As an illustration, we carried out a systematic study of all even-even nuclei having $Z \leq 108$ and $N \leq 184$. We focused our discussion on the drip line systems, finding that in several regions of the periodic table there exist nuclei that are stable against one-particle emission but unstable against pair emission. In the description of very weakly bound systems, small changes of the effective interaction and the many-body treatment can have important consequences, determining, for example, the precise location of the drip lines. Thus, it is important to continue to improve the current HFB+THO methodology to accommodate effects not presently being included. Particularly important is the restoration of symmetries, either exact or approximate.

Acknowledgments

This work has been supported by the U.S. Department of Energy under Contract Nos. DE-FG02-96ER40963 (University of Tennessee), DE-AC05-00OR22725 with UT-Battelle, LLC (Oak Ridge National Laboratory), and DE-FG05-82ER40361 (Joint Institute for Heavy Ion Research), by the Polish Committee for Scientific Research (KBN) under Contract No. 5 P03B 014 21, and by the Interdisciplinary Centre for Mathematical and Computational Modeling (ICM) of the Warsaw University.

References

1. E. Roeckl, Rep. Prog. Phys. **55**, 1661 (1992).
2. A. Mueller and B. Sherril, Annu. Rev. Nucl. Part. Sci. **43**, 529 (1993).
3. P.-G. Hansen, Nucl. Phys. **A553**, 89c (1993).
4. J. Dobaczewski and W. Nazarewicz, Phil. Trans. R. Soc. Lond. A **356**, 2007 (1998).
5. A. Bulgac, Preprint FT-194-1980, Central Institute of Physics, Bucharest, 1980, nucl-th/9907088.
6. J. Dobaczewski, H. Flocard, and J. Treiner, Nucl. Phys. **A422**, 103 (1984).
7. J. Dobaczewski, W. Nazarewicz, T.R. Werner, J.-F. Berger, C.R. Chinn, and J. Dechargé, Phys. Rev. **C53**, 2809 (1996).
8. J. Terasaki, H. Flocard, P.-H. Heenen, and P. Bonche, Nucl. Phys. **A621**, 706 (1997).

9. V.E. Oberacker and A.S. Umar, Proc. Int. Symp. on *Perspectives in Nuclear Physics*, (World Scientific, Singapore, 1999), Report nucl-th/9905010.
10. D. Gogny, Nucl. Phys. **A237**, 399 (1975).
11. M. Girod and B. Grammaticos, Phys. Rev. **C27**, 2317 (1983).
12. J.L. Egido, H.-J. Mang, and P. Ring, Nucl. Phys. **A334**, 1 (1980).
13. J.L. Egido, J. Lessing, V. Martin, and L.M. Robledo, Nucl. Phys. **A594**, 70 (1995).
14. P. Ring, Prog. Part. Nucl. Phys. **37**, 193 (1996).
15. M.V. Stoitsov, J. Dobaczewski, P. Ring, and S. Pittel, Phys. Rev. **C 61** (2000) 034311.
16. M.V. Stoitsov, P. Ring, D. Vretenar, and G.A. Lalazissis, Phys. Rev. **C58**, 2086 (1998).
17. M.V. Stoitsov, W. Nazarewicz, and S. Pittel, Phys. Rev. **C58**, 2092 (1998).
18. M.V. Stoitsov, J. Dobaczewski, W. Nazarewicz, and S. Pittel, Proceedings of the XXI International Workshop on Nuclear Theory, Heron Press, Sofia (2002), pp. 176-192.
19. I.Zh. Petkov and M.V. Stoitsov, Compt. Rend. Bulg. Acad. Sci. **34**, 1651 (1981); Theor. Math. Phys. **55**, 584 (1983); Sov. J. Nucl. Phys. **37**, 692 (1983); Ann. Phys. (NY) **184**, 121 (1988).
20. I.Zh. Petkov and M.V. Stoitsov, *Nuclear Density Functional Theory*, Oxford Studies in Physics, (Clarendon Press, Oxford, 1991).
21. P. Ring and P. Schuck, *The Nuclear Many-Body Problem* (Springer-Verlag, Berlin, 1980).
22. F. Pérez-Bernal, I. Martel, J.M. Arias, and J. Gómez-Camacho, Phys. Rev. **A63**, 052111 (2001).
23. E. Chabanat, P. Bonche, P. Haensel, J. Meyer, and F. Schaeffer, Nucl. Phys. **A635**, 231 (1998).